

Viscous friction in standard rotational motion experiments

M Kovaľaková , M Kladivová, O Fričová, Z Gibová,
M Hutníková and J Kecer

Department of Physics, Faculty of Electrical Engineering and Informatics, Technical University of Košice, Košice 042 00, Slovakia

E-mail: maria.kovalakova@tuke.sk

Received 12 August 2019, revised 9 January 2020

Accepted for publication 27 January 2020

Published 16 March 2020



CrossMark

Abstract

The results of standard experiments demonstrating relationships between dynamic (torque, moment of inertia) and kinematic (angular acceleration) characteristics of rotational motion can provide information on viscous friction acting on the rotating system. The standard experiments presented in this paper were performed using a symmetrical horizontal rotator with changeable moment of inertia (a bar with a symmetrically positioned pair of disc weights) supplied with optical gate; the rotator was driven by a permanent external torque in a resisting ambient atmosphere. The data were processed using the least squares method. The sums of squares of the residuals from the best-fit line (chiSquare values) were used to find out which experiments were influenced by laminar airflows and when turbulent airflows could occur along part of the rotating bar. The proposed experiment can be included in laboratory experiments in bachelor study programmes at colleges and technical universities.

Keywords: rotational motion, viscous friction, laminar airflow

(Some figures may appear in colour only in the online journal)

1. Introduction

Circular and rotational motions are included in basic physics courses at colleges and technical universities. This topic is not very popular among students, since they often find it difficult to grasp the concepts of this kind of motion (angular displacement, angular speed, angular acceleration, torque, and moment of inertia) and the relationships between them. Several studies have dealt with students' misconceptions in this area of physics [1–3]. For this reason experiments demonstrating circular and rotational motions in lectures and/or experiments

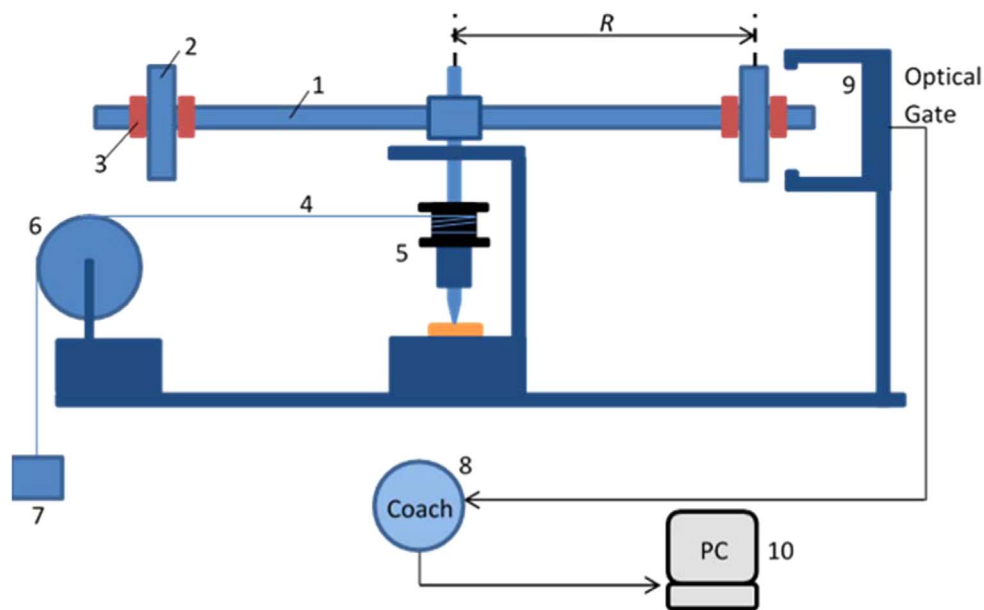


Figure 1. Scheme of the experimental set-up consisting of a 3B Rotational Motion Apparatus 1006 785 [4] and supporting equipment (adapted from [6]).

included in laboratory experiments are a useful tool which can help students in understanding this motion.

The experiment presented in this paper was carried out using commercially available rotation apparatus (3B Scientific [4]). The obtained results, besides illustrating standard relationships between angular acceleration, torque and moment of inertia, reveal that friction forces, both dry (constant) as well as viscous (velocity-dependent, though small and usually neglected), do play a role in this kind of motion, as already reported in [5–9]. The proposed data processing using SciDAVis 1.D013 free software [10], which provided chiSquare values [11], enables us to find out which experiments are influenced by laminar airflows and when turbulent airflows occur [12] along part of the rotating bar depending on the Reynold's number value [13]. Parameters related to laminar friction torque and its relation to the experiment geometry were also obtained.

2. Experimental set-up

Our experiment consisted of recording the values of angular displacement in time for increasing values of the moment of inertia of a rotating bar, with two disc weights placed symmetrically at varying distances from the axis of rotation.

The apparatus depicted in figure 1 consists of a hollow aluminium rod with length 60.0 cm, mass 58.17 g (1), a 200 g disc weight (2), plastic weight fasteners (3) of mass 10.32 g, a length of cord (4), a spindle with radius 9 mm, (5), a pulley (6) and a 50 g slotted weight (7). The force of the driving weight is transferred via the pulley and the cord wrapped around the spindle on the axis of the bar. The moment of inertia of the system can be altered by changing the distance of the disc weights (2), while the torque acting on the system is directly proportional to the mass of the driving weight (7) used. A Coach panel (8), CMA

Photogate code 0662I optical gate (9) and computer (10) make it possible to record the number of half-revolutions (i.e. angular displacement) as a function of time during rotational motion of the system, and to process the experimental data using Coach software. The optical gate enables the recording of the time and angular displacement with accuracy ± 0.01 s and ± 0.01 rad, respectively.

The standard experiments which can be performed using this apparatus enable students to determine the angular acceleration α as a function of torque τ , which sets the bar into motion, and to determine the moment of inertia I as a function of the distance R of the disc weights with mass $2m_d$ from the axis of rotation. The apparatus also makes it possible to perform measurements which provide information on the friction forces acting on the rotational motion of a rigid body [6].

3. Theory

3.1. Rotation apparatus subjected to constant torque of external forces

The rotating apparatus can be considered as a system of bodies (figure 1) with the weight m descending with acceleration of magnitude a and the bar with discs rotating with angular acceleration α for which it holds $a = r\alpha$ where r is the spindle radius. The equations of motion of this system have the following form [6]:

$$\begin{aligned} ma &= mg - T \\ I\alpha &= rT - M_f \end{aligned} \quad (1)$$

where T is the tension in the cord, M_f is the friction torque and I is the moment of inertia

$$I = I_0 + 2m_d R^2 \quad (2)$$

where $I_0 \approx \frac{1}{12}m_{\text{bar}}l_{\text{bar}}^2$ is the moment of inertia of the hollow rod, m_d is the mass of the disc weight with plastic fasteners, R is its distance from the axis of rotation, m is the mass of the driving weight, and r is the spindle radius.

Rearranging equation (1) and taking into account that the term mr^2 can be neglected due to its small value (with respect to the values of I_0 and $2m_d R^2$ for the experimental set-up used), we obtain

$$I\alpha = mgr - M_f. \quad (3)$$

Assuming the constant torque $\tau = mgr - M_f$ on the right side of equation (3) (i.e. there is only dry friction due to sliding of the spindle), the inverse value $1/\alpha$ can be expressed as

$$\frac{1}{\alpha} = \frac{I_0 + 2m_d R^2}{mgr - M_f} \quad (4)$$

which is a linear function with respect to R^2

$$\frac{1}{\alpha} = CR^2 + D \quad (5)$$

where

$$C = \frac{2m_d}{mgr - M_f}, \quad D = \frac{I_0}{mgr - M_f}. \quad (6)$$

The results of experiments with driving weight of mass m , at different distances R of disc weights from the axis of rotation, should demonstrate as follows from equation (5) the linear dependence of $1/\alpha$ on the squared distances R^2 .

The parameters C and D of a straight line fitted to the experimental data can provide the value of friction torque and the moment of inertia of the hollow rod I_0 of the rotation apparatus, as follows from equation (6):

$$M_f = mgr - \frac{2m_d}{C}, I_0 = 2m_d \frac{D}{C}. \quad (7)$$

The values of angular acceleration α for each distance R of disc weights can be obtained by recording the number of half-revolutions n as a function of time, which is related to the angular displacement φ [5]

$$\varphi(t) = \pi n(t) \quad (8)$$

and fitting the theoretical function

$$\varphi = \frac{1}{2}\alpha t^2 + \omega_0 t + \varphi_0 \quad (9)$$

to the experimental data $\varphi(t)$. The disadvantage of this kind of experiment is that the φ values are not recorded at equidistant time intervals. Besides this, in the first phase of the experiment, the problem of static dry friction has to be overcome, which makes this phase sensitive to any external influence. For this reason we also included in the fitting procedure initial angular velocity ω_0 and initial angular displacement φ_0 . The use of a position sensor for this kind of experiment would be more appropriate although taking into account the accuracy of the measurements of time and angular displacement the estimate of relative experimental error for α values is quite low—about 1%.

3.2. Rotation apparatus subjected to dry and viscous friction torques

The flow past a finite and infinite circular cylinders has been the subject of numerous studies [12–16]. In general the flow over a circular cylinder depends on the flow speed u , cylinder diameter d , and kinematic viscosity ν . The flow can be characterized by the dimensionless Reynolds number

$$\text{Re} = \frac{ud}{\nu}. \quad (10)$$

The Reynolds number makes it possible to distinguish between laminar (for Re up to the order of 10^2) and turbulent flows (Re above 10^4) past a circular cylinder [16].

However, the rotating bar is a circular cylinder in the flow with linear speed increasing from zero at the axis of rotation to the maximum value at the bar end. For this reason, the exact Reynolds numbers for a rotating bar with disc weights at various positions should be determined experimentally.

If the linear velocities u along a rotating bar length are sufficiently low then the airflow is laminar, but if they are high enough ($\omega r > u_{cr}$ for $r > r_{cr}$) at a certain distance r_{cr} from the axis of rotations at which the Reynolds number acquires its critical value [12, 13, 16], then the airflow is turbulent. The profile of linear velocities of a bar (circular cylinder) rotating with angular velocity ω is qualitatively depicted in figure 2.

The motion of the rotating bar could therefore be simultaneously influenced by laminar and turbulent viscous forces depending on the value of bar angular velocity. The friction

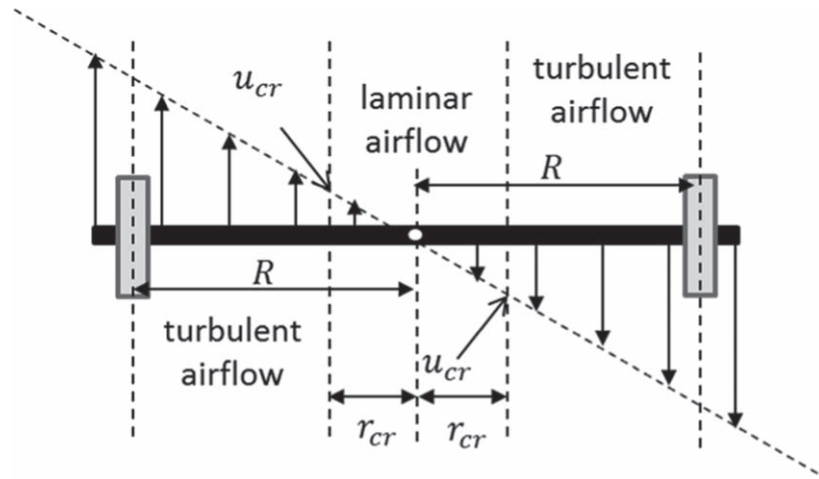


Figure 2. Profile of linear velocities of a rotating bar; $u_{cr} = r_{cr}\omega$ is critical linear velocity, R —distance of disc weights from axis of rotation.

torque M_f acting on the rotating bar can be expressed as

$$M_f = f_0 + M_{f_{\text{lamin}}} + M_{f_{\text{turb}}} \quad (11)$$

where f_0 is the dry friction torque, and $M_{f_{\text{lamin}}}$ and $M_{f_{\text{turb}}}$ are friction torques related to laminar and turbulent airflows respectively.

During uniformly accelerated motion both kinds of viscous forces could be present. The critical r_{cr} distance in the beginning of each experiment is larger than the bar radius (the whole bar is in a laminar airflow). At a sufficiently high angular velocity this critical distance r_{cr} starts decreasing and both regions with turbulent (the bar ends) and laminar (close to the axis of rotation) airflows are present. The solution of the equation of motion taking into account both viscous contributions (equation (11)) requires quite a complex expression and its solution is beyond the scope of bachelor study programs. However, for small enough angular velocities ω , the contribution of turbulent viscous friction torques can be neglected and the friction torque can be expressed (as follows from the Navier–Stokes equation [12]) as

$$M_f = f_0 + f_1\omega \quad (12)$$

where $f_1\omega = M_{f_{\text{lamin}}}$ and f_1 is the parameter related to the laminar viscous friction torque.

In this case the equation of motion (equation (3)) has the form

$$I\alpha = mgr - f_0 - f_1\omega. \quad (13)$$

Rearranging equation (13) and taking into account that $\alpha = \frac{d\omega}{dt}$, we obtain

$$\frac{d\omega}{dt} = A - B\omega \quad (14)$$

where

$$A = \frac{mgr - f_0}{I} \quad (15)$$

$$B = \frac{f_1}{I}. \quad (16)$$

The solution of equation (14) provides the following formulae for angular velocity ω and angular displacement φ :

$$\omega = \frac{A}{B} + \left(\omega_0 - \frac{A}{B} \right) \exp(-Bt) \quad (17)$$

$$\varphi = \frac{A}{B}t + \frac{\omega_0 B - A}{B^2}(1 - \exp(-Bt)) + \varphi_0. \quad (18)$$

The I values can be calculated using equation (2) and the value $2m_d = 0.41032$ kg, which also includes the mass of the plastic weight fasteners, and using equations (15), (16), (18) the friction forces can be evaluated.

4. Experimental results and discussion

4.1. Outline of the experiment and data processing

- The measurements were carried out for 25 values of the distance R , and the experiment for each R value was repeated three times. Since the rotation apparatus is placed on a laboratory table, the length of cord (4) is limited by the height of the table, and the number of half-revolutions is constant for all measurements.
- A polynomial of the second order (equation (9)) was fitted to the recorded dependences $\varphi = f(t)$, and these fits were assessed using chiSquare (χ^2) values. The α values from the experiments with the lowest chiSquare (χ^2) values were used in the next task.
- On the assumption that friction torque is constant, the inverse values of angular acceleration $1/\alpha$ are expected to be a linear function of the R^2 (equation (5)). The parameters obtained from fitting a straight line to the plot $1/\alpha = f(R^2)$ made it possible to calculate the friction torque and the moment of inertia of the rotating bar (equation (7)).
- The contribution from viscous friction torque acting on the rotating part of the apparatus was obtained as the difference between the friction torque M_f calculated using equation (7) and the dry friction torque f_0 (estimated from the minimum mass attached to the cord which is needed to start the rotational motion of the cross bar [6]).
- The chiSquare (χ^2) values were used to assess the fits of theoretical functions equation (18) which take into account not only dry but also laminar friction torques acting on the rotating system, to experimental data. The χ^2 values gave information regarding in which experiments the viscous forces could be neglected, which experiments were influenced by laminar airflows, and when turbulent airflow was possibly present.
- Processing the data from the experiments in which turbulent airflow was possibly not present provided the values of the parameter f_l related to laminar friction torque (see equations (15), (16), (18)) and its relation to the geometry of the rotating system (the positions R of m_d).

4.2. Results obtained on the assumption of constant friction torque

The fits of equation (9) to the measured values of angular displacement φ obtained in three experiments for each R value were assessed by means of the chiSquare values. The inverse values of angular acceleration were calculated for the experiments with the lowest χ^2 values (from three experiments). The plot of $1/\alpha$ against squared distances R^2 of the disc weights from the axis of rotation can be seen in figure 3. (The relative errors of α values determined in

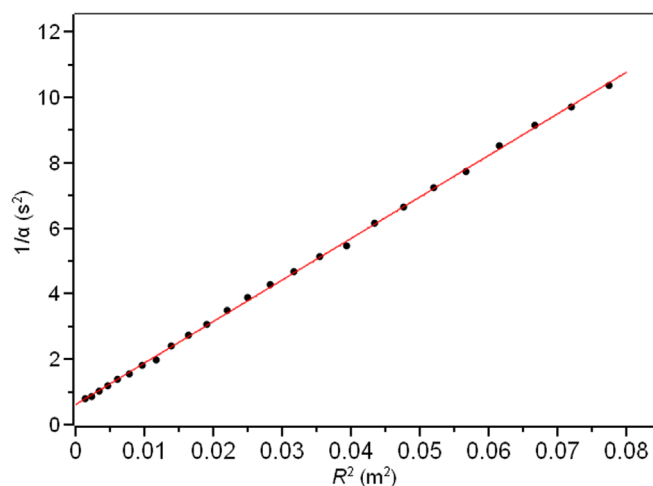


Figure 3. Inverse values of angular acceleration (solid symbols) versus squared distance of disc weights from the axis of rotation with a fitted straight line (solid line).

the fitting procedure using the SciDAVis program were smaller than 1% and the plotted intervals are within the solid symbols in figure 3.)

Using the parameters $C = 126.90 \text{ s}^2 \text{ m}^{-2}$, $D = 0.6068 \text{ s}^2$ of the fitted straight line and equation (7), the values 0.00196 kgm^2 and $11.81 \times 10^{-4} \text{ Nm}$ were calculated for the moment of inertia I_0 and the friction torque M_f respectively.

The moment of inertia of the hollow rod can be calculated using the theoretical expression for the moment of inertia $I_{0 \text{ theor}}$ of a bar of mass m and length l_{bar} rotating about an axis through its centre of mass: $I_{0 \text{ theor}} = \frac{1}{12} m_{\text{bar}} l_{\text{bar}}^2 = \frac{1}{12} 0.05817 \times 0.60^2 = 0.00175 \text{ kgm}^2$. The value 0.00196 kgm^2 obtained from the experimental data is close to this value.

The value of friction torque $11.81 \times 10^{-4} \text{ Nm}$, which is larger than the value $4.19 \times 10^{-4} \text{ Nm}$ of dry friction for this apparatus [6], is an indication that viscous friction torque, which averaged value is $7.62 \times 10^{-4} \text{ Nm}$, acts on the rotating bar with disc weights. It is worth noting that viscous friction torque is small with respect to the driving weight torque (mgr) which is $44.15 \times 10^{-4} \text{ Nm}$. Average angular velocity in each particular experiment decreases with increasing R value (due to the constant number of half-revolutions in each experiment mentioned above, i.e. smaller maximum velocity for higher R values). For this reason a larger contribution of the viscous friction torque can be expected in measurements for smaller R values.

4.3. Results obtained on the assumption of the presence of laminar friction torque

The maximum angular velocity of the rotating bar in our experiments ($d = 0.008 \text{ m}$, $\nu = 14.88 \times 10^{-6} \text{ m}^2 \text{ s}^{-1}$ [17]) was from 3.1 to 10.8 s^{-1} i.e. the Reynolds numbers (calculated using equation (10)) for the end of the rotating bar (radius 0.3 m) in the range from 500 to 1740 . Disc weights with a diameter of 5 cm have Reynolds number approximately six times higher than the rotating bar. Due to the relatively small height of the disc weights (1.37 cm) with respect to the length of the rotating bar (0.6 m), their contribution to friction torque could be expected to be small.

The fits of the function (equation (18)), which takes into account laminar friction torque, to the experimental data were evaluated using the χ^2 values for each position (R) of the disc weights

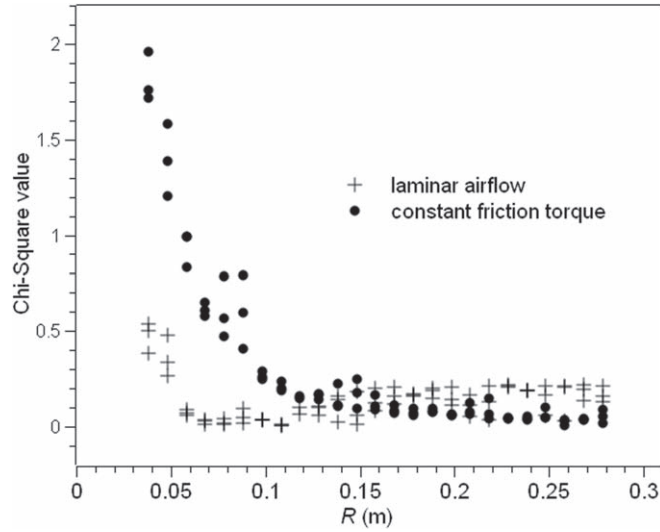


Figure 4. χ^2 values for the fitting of equations (9) and (18) to the experimental data obtained for different R distances of disc weights from the axis of rotation.

(figure 4). The A parameter was calculated using equation (15) ($f_0 = 4.19 \times 10^{-4}$ Nm [6], and I calculated using equation (2)) was kept constant in the fitting procedure, which provided parameters B and φ_0 . As can be seen in figure 4 a good agreement, i.e. low χ^2 values, between the experimental and fitted values was obtained for R values larger than 0.06 m. Below this value, at higher average velocities (smaller moments of inertia), i.e. higher Reynolds number, χ^2 values are considerably higher, which means that airflow flow is not more only laminar but turbulent friction torque is present at least at the end parts of the rotating bar.

For comparison, χ^2 values of the fitting of equation (9), which corresponds to constant friction torque, to the experimental data are also plotted in figure 4. Low χ^2 values were obtained for R distances larger than 0.15 m, which means for low values of angular velocities (high values of the moment of inertia) when the contribution of laminar friction torque is relatively small. For this plot rather poor agreement between experimental and fitted values is observed for R distances lower than 0.12 m (higher angular velocities) when both laminar and turbulent airflows could be present.

Taking into account the results plotted in figure 4 it can be concluded that

- for $R < 0.06$ m the end parts of the rotating bar are influenced by turbulent airflow;
- for $R > 0.06$ m the system is in laminar airflow;
- for $R > 0.12$ m the influence of viscous forces is so small that the friction torque can be presumed constant, and χ^2 values for the fits of equations (9) and (18) overlap.

The values of the f_1 parameter related to laminar airflow were calculated using equation (16) for each R value. The f_1 values were determined with relative error smaller than 1%. As can be seen in figure 5 they depend on the R value.

The effect of the position of the disc weights on parameter f_1 is due to greater contribution of the disc weights to the resulting friction torque (equation (11)) at increasing R distances

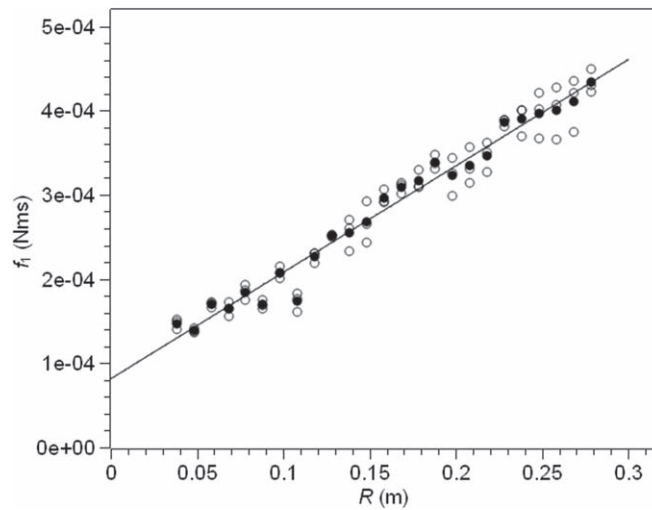


Figure 5. Plot of parameter f_1 related to laminar viscous friction torques versus the R distance of the disc weights from the axis of rotation (open symbols) and the mean f_1 values for each R distance (solid symbols).

$$M_f = f_0 + (f_1' + Rf_1'')\omega \quad (19)$$

where $f_1' + Rf_1'' = f_1$ and f_1', f_1'' are parameters related to the bar and disc weights at distance R from the axis of rotation in laminar airflow.

The intercept of the linear dependence $f_1' = 0.81 \times 10^{-4}$ Nms can be then considered as the parameter related to the rotating bar with disc weights placed in the axis of rotation.

5. Conclusion

This series of standard rotational motion experiments was performed on commercially available rotation apparatus with constant external torque and increasing moment of inertia of the rotating parts, due to increasing distance of the disc weights from the axis of rotation. The values of angular displacement were recorded in real time using the Coach system and an optical gate.

The plots of inverse values of angular acceleration versus squared distance of the disc weights from the axis of rotation made it possible

- to assess the values of the moment of inertia of the rotating bar and the friction torque acting on the apparatus in the series of measurements; and
- to deduce the presence of viscous forces from the difference between the values of the friction torque obtained and dry friction torque.

The fitting of theoretical functions $\varphi(t)$ to the experimental data taking into account the influence of laminar viscous friction torque or presumed constant friction torque made it possible

- to infer from the chiSquare values in which experiments turbulent airflow is present;
- to find the parameters related to laminar airflow for the apparatus used; and
- to assess the dependence of the laminar friction parameters on the position of the disc weights.

The proposed experiments can help students to improve their knowledge of the friction forces acting on the rotational apparatus. Moreover, students can see the usefulness of chiSquare values in evaluating the appropriateness of the models used for the interpretation of experimental data.

ORCID iDs

M Kovařáková  <https://orcid.org/0000-0002-8104-4536>

References

- [1] López M L 2003 Angular and linear acceleration in a rigid rolling body: students' misconceptions *Eur. J. Phys.* **24** 6
- [2] Rimoldini L G and Ch S 2005 Student understanding of rotational and rolling motion concepts *Phys. Rev. Special Topics—Phys. Edu. Res.* **1** 010102
- [3] Mashood K K and Singh V A 2012 An inventory on rotational kinematics of a particle: unravelling misconceptions and pitfalls in reasoning *Eur. J. Phys.* **33** 5
- [4] 3B Scientific 2020 Rotational Motion Apparatus 1006785, Instruction sheet (https://3bscientific.com/product-manual/1006785_EN.pdf)
- [5] Gibová Z, Fričová O, Kladivová M, Kecer J, Hutníková M and Kovařáková M 2016 Rotational motion of a rigid body with the system IP–Coach *Phys. Educ. (India)* **32** 4
- [6] Kladivová M, Kovařáková M, Gibová Z, Fričová O, Hutníková M and Kecer J 2016 Laboratory experiment for the study of friction forces using rotating apparatus *Eur. J. Phys.* **37** 6
- [7] Eadkhong T, Rajsadorn R, Jannual P and Danworaphong S 2012 Rotational dynamics with Tracker *Eur. J. Phys.* **33** 615–22
- [8] Alam J, Hassan H, Shamim S, Mahmood W and Anwar M S 2011 Precise measurement of velocity dependent friction in rotational motion *Eur. J. Phys.* **32** 1367–75
- [9] Mungan C E 2012 Frictional torque on a rotating disc *Eur. J. Phys.* **33** 1119–23
- [10] SciDAVis 2019 1.D013 (<https://sourceforge.net/projects/scidavis/files/SciDAVis/1.D13/>)
- [11] Vasilief I, Gadiou R, Franke K, Nascimento F and Garriga M 2018 The SciDAVis Handbook (<https://usermanual.wiki/Document/scidavismanual20180625.1951139997.pdf>)
- [12] Landau L D and Lifshitz E M 1987 *Fluid Mech.* vol 6 Course of Theoretical Physics, Second English edition, Revised (Oxford: Pergamon) pp 61 and 180
- [13] Zdravkovich M 1997 *Flow Around Circular Cylinders* vol 1 (Oxford: Oxford University Press)
- [14] Rajani B N, Kandasamy A and Majumdar S 2009 Numerical simulation of laminar flow past a circular cylinder *Appl. Math. Modell.* **33** 1228–47
- [15] Hamane D, Guerri Q and Larbi S 2014 Investigation of flow around a circular cylinder in laminar and turbulent flow using the Lattice Boltzmann Method *AIP Conf. Proc.* **1648** 850094-1–4 (<https://aip.scitation.org/doi/abs/10.1063/1.4913149>)
- [16] Feynman Richard, Leighton Robert and Sands Matthew 2010 *The Feynman Lectures on Physics: New Millennium Edition* ed M A Gottlieb and R Pfeiffer vol 2 (Pasadena, CA: California Institute of Technology) ch 4 (https://feynmanlectures.caltech.edu/II_41.html)
- [17] Dixon J C 2007 Appendix B: Properties of Air *The Shock Absorber Handbook* 2nd edn (Chichester: Wiley)